7 BCFW recursion for loops

The unitarity cuts discussed in Chapter 6 involve cuts of *at least two* propagators. In contrast, the tree-level recursion relation of Chapter 3 looks more like a single-line cut construction, since it uses the factorization-structure of a single propagator going on-shell. It is tempting to ask if loop amplitudes can similarly be reconstructed from the singularities associated with taking a single propagator on-shell. In this chapter, we study a recursive approach that generalizes the tree-level BCFW construction to loop-integrands.

We begin in Section 7.1 with a discussion of what is meant by *the* loop-integrand of an amplitude and how and when it is well-defined. The rest of the chapter focuses on super-BCFW recursion relations for loop-integrands of planar superamplitudes in $\mathcal{N} = 4$ SYM. In this setting it is quite natural to work with the momentum twistor variables introduced in Section 5.4; we will in particular make use of the description given there of points, lines, and planes in momentum twistor space. It is interesting how the description of the BCFW shift becomes geometric in the momentum twistor description, for example, the on-shell conditions for the internal line in a diagram become a statement of intersection of lines and planes. We demonstrate the geometrization in Section 7.2 and apply it in Section 7.3 to derive the super-BCFW result for the N^kMHV tree-level superamplitude in $\mathcal{N} = 4$ SYM. Thence, suitably warmed up and prepared, we introduce loop-recursion in Section 7.4. In Section 7.5, we give a fully worked-through example of its application to the 4-point 1-loop superamplitude of $\mathcal{N} = 4$ SYM. We end with brief comments about higher loop amplitudes in Section 7.6.

7.1 Loop-integrands

As seen in Chapter 6, loop amplitudes have a complicated analytic structure, so we focus on the *loop-integrand* which is just a rational function with poles at the location of the propagators, much similar to the tree amplitudes. Suppose we do a BCFW shift on the external legs, for example $p_1^\mu \to p_1^\mu + z\, q^\mu$ and $p_n^\mu \to p_n^\mu - z\, q^\mu$, with $q^2 = 0$ as usually. We can deduce from the Feynman diagrams that the shifted loop-integrands possess two types of poles in z:

1. poles in loop-independent propagators;
2. poles in propagators involving loop-momentum.

Downloaded from https://www.cambridge.org/core. UNIVERSIDAD AUTONOMA METROPOLITANA, on 14 Nov 2026 at 01:30:40, subject to the Cambridge Core terms of use, available at https://www.cambridge.org/core/terms. https://doi.org/10.1017/CBO9781107706620.010

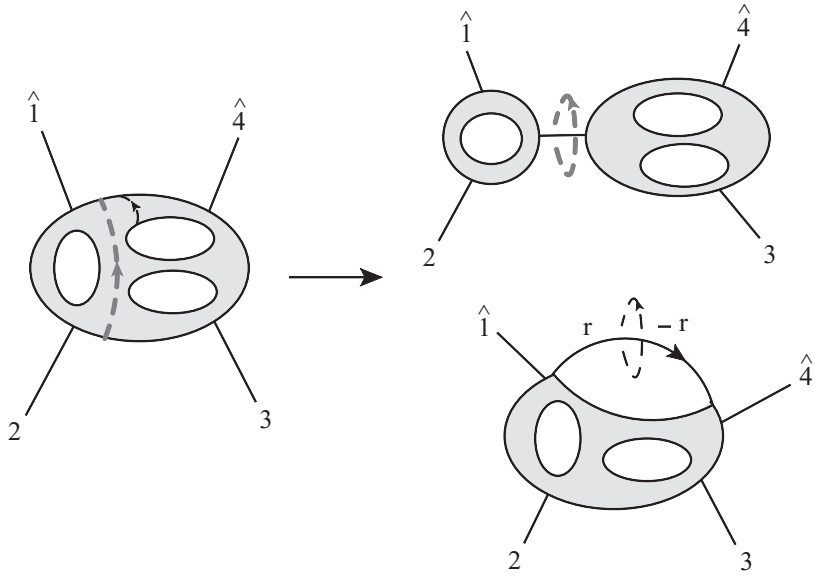


Fig. 7.1 Representation of the two types of poles occurring in a BCFW shift of a 4-point 3-loop integrand. Type 1 are poles associated with loop-momentum *independent* propagators and type 2 poles are loop-momentum *dependent* propagators. The former factorizes the 3-loop integrand into a product of a 2-loop and a 1-loop integrand while the latter gives a forward limit of a 2-loop amplitude with two extra legs.

The residue of a type 1 pole corresponds to factorization of the integrand into a product of two lower-loop integrands. The residue of a type 2 pole in an L-loop n-point integrand is an $(n+2)$-point $(L-1)$-integrand with two adjacent legs evaluated in the ***forward limit***

$$p_i^\mu \to r^\mu\,, \qquad p_{i+1}^\mu \to -r^\mu\,, \quad \text{with} \quad r^2 = 0\,. \tag{7.1}$$

This is illustrated for the example of a 4-point 3-loop amplitude in Figure 7.1. The poles of type 2 are what we would call single-line cuts in the unitarity method [113, 114].

Thus – provided that the large-z behavior is well-understood – it appears that one can straightforwardly set up a recursion relation for loop-integrands. However, there are subtleties we have to resolve:

- The first issue has to do with the identification of the loop-momenta in the loop-integrand. In the amplitude, we have to integrate the loop-momenta, so the ℓ_i are just dummy variables that can be redefined while still giving the same integrated answer. But the integrand itself can have different pole structures depending on how the ℓ_i are identified. As an example, consider the 1-loop 4-point box-integral (6.1) and compare the equivalent parameterizations $I_4^{(a)}$ and $I_4^{(b)} = I_4^{(a)}(\ell \to \ell + p_1)$. BCFW shifting legs 1 and 2 yields

Downloaded from https://www.cambridge.org/core. UNIVERSIDAD AUTONOMA METROPOLITANA, on 14 Nov 2026 at 01:30:40, subject to the Cambridge Core terms of use, available at https://www.cambridge.org/core/terms. https://doi.org/10.1017/CBO9781107706620.010

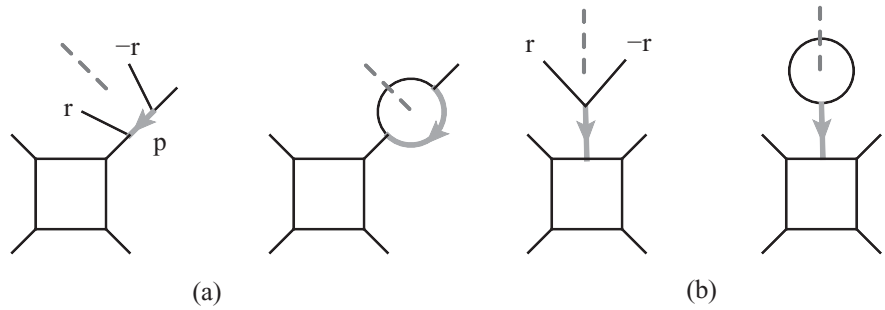


Fig. 7.2 Examples of diagrams problematic for the forward limit. In the lefthand diagram of (a), the propagator between the forward legs diverges due to momentum conservation. The righthand part of diagram (a) illustrates that such a diagram corresponds to the single-cut of a bubble on an external leg. Similar remarks apply to the diagrams in (b), where the limit corresponds to cutting a tadpole.

two distinct analytic functions in z:

$$I_4^{(a)}(\hat{1},\hat{2},3,4) = \frac{1}{\ell^2(\ell - p_1 - z\,r)^2(\ell - p_1 - p_2)^2(\ell + p_4)^2}\,,$$
$$I_4^{(b)}(\hat{1},\hat{2},3,4) = \frac{1}{(\ell + p_1 + z\,r)^2\ell^2(\ell - p_2 + z\,r)^2(\ell - p_2 - p_3 + z\,r)^2}\,. \tag{7.2}$$

In general there is no canonical way to identify how the loop-momentum is parameterized, so that is the first subtlety that needs to be resolved. It basically comes down to the definition of what we mean by *the* "un-integrated integrand."

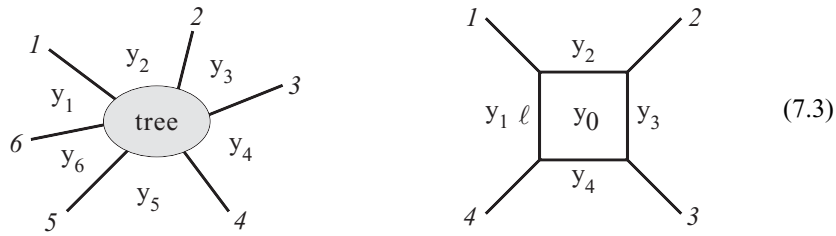
- The second subtlety has to do with the forward limit (7.1). When loop-momentum-dependent propagators go on-shell, there is a residue corresponding to a lower-loop $(n+2)$-point integrand in the forward limit, but that limit suffers from singularities. For example, from the explicit Feynman diagrams one sees that if the forward legs are attached to the same external line, then due to momentum conservation there is a $1/p^2$ singularity as $p^2 \to 0$. Such diagrams can be identified with cuts of bubbles on external legs or tadpole diagrams. This is illustrated in Figure 7.2. In massless theories, these integrate to zero in dimensional regularization and do not contribute to the loop amplitude. However, prior to integration, they are part of the integrand and will contribute to the single cuts. Therefore an important, but difficult, task is to identify these contributions in the forward limit such that one can consistently remove them.

Resolution of the above subtleties has been partially achieved for non-supersymmetric theories [113] and *completely resolved in supersymmetric theories in the planar limit* [114, 115]. In particular, it was shown that for supersymmetric theories the problematic terms associated with the tadpole as well as for external bubbles cancel in the state sum over the supermultiplet, and thus one has a perfectly well-defined residue. Furthermore, in the planar limit, the loop-momenta in the integrand can be defined unambiguously. This is done by defining the ℓ_is with a specific relation to the ordering of the external momenta. For example at 1-loop, one choice is to declare that ℓ is the momentum associated with

Downloaded from https://www.cambridge.org/core. UNIVERSIDAD AUTONOMA METROPOLITANA, on 14 Nov 2026 at 01:30:40, subject to the Cambridge Core terms of use, available at https://www.cambridge.org/core/terms. https://doi.org/10.1017/CBO9781107706620.010

the internal line immediately before line 1. For the 4-point 1-loop box integral, this selects integrand $I_4^{(a)}$ in (7.2).

The identification of the loop-momentum is naturally done in dual space y, that we defined in (5.31) in order to make momentum conservation manifest. We noted there that the y_is are also sometimes called zone variables; that is because we can think of them as labeling the "zones," or regions, that the external lines of the amplitude separate the plane into. This assumes a well-defined ordering of the external lines based on the color-ordering – and at loop-level it further requires the graphs to be planar. Let us illustrate this for a 6-point tree-graph and the 4-point 1-loop box diagram:



(7.3)

At loop-level there are "internal" zones, one for each loop. This offers the opportunity to switch the integration variable from ℓ_i to the new internal zone variables. For example in the 4-point 1-loop box graph, we can use y_0 as the loop-parameter instead of ℓ. They are related by $\ell = y_1 - y_0$, similarly to the relationship $p_i = y_i - y_{i+1}$. The dual variables therefore give an unambiguous definition of the loop-momentum and this facilitates the loop-level recursion relations for planar integrands.

As a useful example, let us express the 4-point scalar box-integral from (7.3) in dual variables. Following the rules for identifying the momentum on each internal line in terms of the zone-variables of the two adjacent zones, we have $\ell_i^2 = (y_0 - y_i)^2 = y_{0i}^2$. The box-integral is therefore simply

$$I_4(p_1, p_2, p_3, p_4) = \int \frac{d^4\ell}{(2\pi)^4} \frac{1}{\ell^2(\ell - p_1)^2(\ell - p_1 - p_2)^2(\ell + p_4)^2} \rightarrow \int \frac{d^4 y_0}{y_{01}^2\, y_{02}^2\, y_{03}^2\, y_{04}^2}\,. \tag{7.4}$$

To reiterate, for *planar amplitudes in supersymmetric theories, all subtleties in defining the loop-integrand have been overcome.* In the following, we introduce a BCFW recursion relation that generates the planar loop-integrands for $\mathcal{N} = 4$ SYM; it was developed in [115] and also considered in [116].

7.2 BCFW shift in momentum twistor space

The planar integrand is well-defined in the dual coordinates y_i, so it would seem natural to formulate the BCFW shifts in the dual representation. However, it is actually more

Downloaded from https://www.cambridge.org/core. UNIVERSIDAD AUTONOMA METROPOLITANA, on 14 Nov 2026 at 01:30:40, subject to the Cambridge Core terms of use, available at https://www.cambridge.org/core/terms. https://doi.org/10.1017/CBO9781107706620.010

interesting to use the momentum supertwistors $\mathcal{Z}_i^{\mathsf{A}}$ that we introduced in Section 5.4. The $\mathcal{Z}_i^{\mathsf{A}}$s can be chosen freely in $\mathbb{CP}^{3|4}$ and make momentum conservation, supermomentum conservation, and on-shell conditions automatic. We can therefore set up the BCFW shift without worrying about these constraints. The simplest possibility is to shift just a single momentum twistor, say $\mathcal{Z}_i$:

$$\hat{\mathcal{Z}}_i = \mathcal{Z}_i + w\mathcal{Z}_{i+1}\,. \tag{7.5}$$

All other $\mathcal{Z}_j$s are unshifted. The shift parameter w is a complex variable, $w \in \mathbb{C}$. Geometrically, (7.5) is the statement that the point $\hat{\mathcal{Z}}_i$ lies on the line $(i, i+1) = (\mathcal{Z}_i, \mathcal{Z}_{i+1})$.[1]

Let us translate (7.5) back to the spinor helicity formalism. In components (7.5) says

$$|\hat{i}\rangle = |i\rangle + w\,|i+1\rangle\,, \qquad |\hat{\mu}_i] = |\mu_i] + w\,|\mu_{i+1}]\,, \qquad \hat{\chi}_{iA} = \chi_{iA} + w\,\chi_{i+1,A}\,. \tag{7.6}$$

Using (5.46) and the incidence relations (5.44), one finds that

$$\hat{y}_i = y_i + z\,|i-1\rangle[i|\,, \tag{7.7}$$

where

$$z = \frac{w\langle i, i+1\rangle}{\langle i-1, i\rangle + w\langle i-1, i+1\rangle}\,. \tag{7.8}$$

All other y_js are unshifted.

▶ **Exercise 7.1**

Use (5.46) and (5.44) to show that y_{i+1} and y_{i-1} are unshifted. Then derive (7.7).

The shift in y-space makes sense geometrically, because by Figure 5.1 the point $\hat{y}_{i+1}$ is determined by the line $(\hat{i}, i+1)$ which is equivalent to the line $(i, i+1)$ since (7.5) exactly tells us that the point $\hat{\mathcal{Z}}_i$ lies on $(i, i+1)$. So we conclude $\hat{y}_{i+1} = y_{i+1}$. On the other hand, $\hat{y}_i$ is determined by the line $(i-1, \hat{i})$ which is different from $(i-1, i)$, so $\hat{y}_i \neq y_i$ for $w \neq 0$.

Translating from dual y-space to momentum space, we have

$$\hat{p}_i = \hat{y}_i - y_{i+1} = -\big(|i\rangle - z|i-1\rangle\big)[i|\,, \tag{7.9}$$

$$\hat{p}_{i-1} = y_{i-1} - \hat{y}_i = -|i-1\rangle\big([i-1| + z[i|\big)\,. \tag{7.10}$$

No other momenta shift. We immediately read off that this is a $[i-1, i\rangle$ BCFW shift,

$$|\hat{i}\rangle = |i\rangle - z|i-1\rangle\,, \qquad |\widehat{i-1}] = |i-1] + z|i]\,. \tag{7.11}$$

Since there is also a shift of the Grassmann-components of the momentum supertwistors, (7.5) actually induces a BCFW $[i-1, i\rangle$-supershift.

▶ **Exercise 7.2**

Show that the Grassmann-part of the shift in (7.5) is equivalent to $\hat{\eta}_{i-1} = \eta_{i-1} + z\,\eta_i$.

[1] As in Section 5.4, we denote the line in momentum twistor space defined by two points (Z_j, Z_k) as (j, k), and the plane defined by three points (Z_j, Z_k, Z_l) as (j, k, l).

Downloaded from https://www.cambridge.org/core. UNIVERSIDAD AUTONOMA METROPOLITANA, on 14 Nov 2026 at 01:30:40, subject to the Cambridge Core terms of use, available at https://www.cambridge.org/core/terms. https://doi.org/10.1017/CBO9781107706620.010

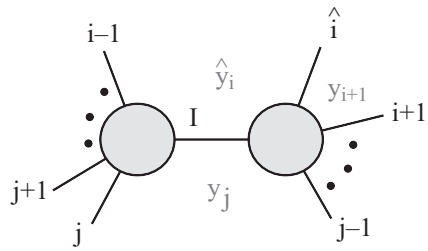
▶ **Exercise 7.3**

It may seem surprising that the shift $\hat{\mathcal{Z}}_i = \mathcal{Z}_i + w\mathcal{Z}_{i+1}$ is equivalent to a $[i-1, i\rangle$-supershift; one might have expected a shift involving lines i and $i+1$ instead. Actually, the shift (7.5) is also equivalent to a $[i+1, i\rangle$ shift: this is because the momentum twistors are defined projectively, so we could supplement (7.5) with an overall scaling. For example, one finds that the angle spinor shift in (7.11) is equivalent to

$$|\hat{i}\rangle = \frac{\langle i-1, i\rangle}{\langle i-1, i\rangle + w\langle i-1, i+1\rangle}\left(|i\rangle + w|i+1\rangle\right). \tag{7.12}$$

Manipulate $|\hat{i}\rangle$ in (7.11) to find (7.12).

Our next task is to describe the kinematics associated with the internal lines in the BCFW diagrams – it turns out to have a nice geometric description in momentum twistor space. Consider a typical BCFW diagram associated with a factorization channel P_I:



(7.13)

For simplicity, let us for now suppose that there are no loop-momenta in P_I. The shifted momentum on the internal line is

$$\hat{P}_I^2 = (\hat{p}_i + p_{i+1} + \cdots + p_{j-1})^2 = (\hat{y}_i - y_j)^2 = \hat{y}_{ij}^2 = \frac{\langle i-1, \hat{i}, j-1, j\rangle}{\langle i-1, i\rangle\langle j-1, j\rangle}. \tag{7.14}$$

In the last step, we have written the distance in dual y-space in terms of the 4-bracket, as in (5.52), and we have also used that $\langle i-1, \hat{i}\rangle = \langle i-1, i\rangle$. The shift $\hat{Z}_i = Z_i + w\, Z_{i+1}$ says that the point $\hat{Z}_i$ lies on the line $(i, i+1)$ and its position on that line is parameterized by w. The condition $\hat{P}_I^2 = 0$ is the statement that w is chosen such that $\langle i-1, \hat{i}, j-1, j\rangle = 0$, so this value w_* is such that the point $\hat{Z}_i$ lies in the plane $(i-1, j-1, j)$. In other words, $\hat{Z}_i$ can be characterized as the point of intersection between the line $(i, i+1)$ and the plane $(i-1, j-1, j)$, viz.

$$(\hat{i}\,) = (i, i+1)\bigcap(i-1, j-1, j). \tag{7.15}$$

The intersection formula was given in (5.66) in terms of the 4-brackets. The geometry is illustrated in Figure 7.3(a).

We now determine the momentum twistor Z_I associated with the internal line $\hat{P}_I$. Take a look at the BCFW diagram in (7.13). The point y_j in dual space can be determined by the line $(j-1, j)$ in momentum twistor space. But by inspection of (7.13), y_j can also be determined by the line (I, j). This means that the three points Z_I, Z_{j-1}, and Z_j lie on the same line. Similarly, the point $\hat{y}_i$ can be determined by the line $(i-1, \hat{i})$ or by the line

Downloaded from https://www.cambridge.org/core. UNIVERSIDAD AUTONOMA METROPOLITANA, on 14 Nov 2026 at 01:30:40, subject to the Cambridge Core terms of use, available at https://www.cambridge.org/core/terms. https://doi.org/10.1017/CBO9781107706620.010

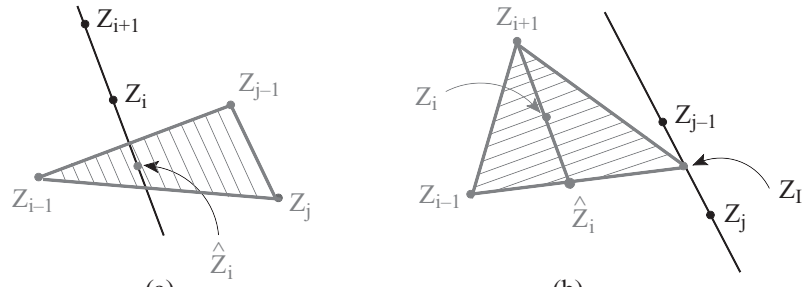


Fig. 7.3 The geometry of (7.15) and (7.16): (a) shows that the on-shell condition $\hat{P}_I^2 = 0$ fixes the shifted momentum twistor $\hat{Z}_i$ to be at the intersection of the line $(i, i+1)$ with the plane $(i-1, j, j-1)$. In (b) the momentum twistor Z_I is located at the intersection of line $(j, j-1)$ and the plane $(i-1, i, i+1)$.

$(I, \hat{i})$, so Z_I, Z_{i-1}, and $\hat{Z}_i$ lie on the same line. Since Z_I lies on both lines, we conclude that Z_I can be characterized as the intersection point of the lines $(i-1, \hat{i})$ and $(j-1, j)$. We previously learned that $\hat{Z}_i$ lies in the plane $(i-1, j-1, j)$, and therefore the plane contains the line $(i-1, \hat{i})$. Thus we conclude that Z_I is the point where the line $(j-1, j)$ intersects the plane $(i-1, i, i+1)$:

$$(I) = (j, j-1) \bigcap (i-1, i, i+1)\,. \tag{7.16}$$

The geometry is shown in Figure 7.3(b). These results will be useful in the following.

Now we are ready to study the BCFW recursion relations in momentum twistor space. Consider the BCFW shift (7.5) of an n-point L-loop integrand $\mathcal{I}_n^L$ (for tree-level you can translate "integrand" to "superamplitude" in your head). The recursion relations are based on the contour argument for $\int \frac{dw}{w} \hat{\mathcal{I}}_n^L(w)$, just as in Section 3.1. Poles at finite values of w are equivalent, via (7.8), to poles at finite z: they arise from propagators with momentum $\hat{y}_{ij}$ going on-shell and the corresponding BCFW diagrams are those in (7.13). However, in completing the contour integral argument we also need to consider the large-w limit. It is clear from the relation (7.8) that z goes to a finite value z_* as $w \to \infty$. Specifically,

$$z \xrightarrow{w\to\infty} z_* \equiv \frac{\langle i, i+1\rangle}{\langle i-1, i+1\rangle}\,. \tag{7.17}$$

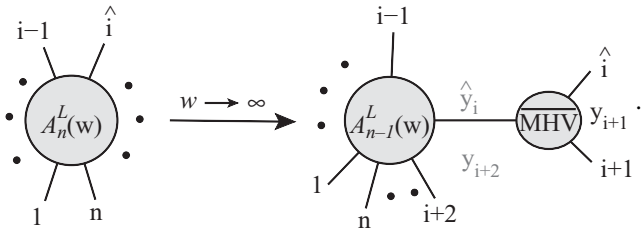
Thus the pole at infinity in the w-plane maps to a finite point in the z-plane and we will have to consider this contribution too. At $w = \infty$, the shifted angle spinors are

$$|\hat{i}\rangle\Big|_{w\to\infty} = \frac{\langle i-1, i\rangle}{\langle i-1, i+1\rangle}\,|i+1\rangle\,. \tag{7.18}$$

Thus, in the limit $w \to \infty$, the spinors $|\hat{i}\rangle$ and $|i+1\rangle$ become proportional, and that implies that $\hat{P}_{i,i+1} = \hat{p}_i + p_{i+1}$ is on-shell: $\hat{P}_{i,i+1}^2 = \langle \hat{i}, i+1\rangle[i, i+1] \to 0$ for $w \to \infty$. Or equivalently, we may note that z_* is exactly the solution to $\langle \hat{i}, i+1\rangle = 0$. Hence the pole at $w = \infty$ corresponds to a factorization channel of an integrand into a 3-point anti-MHV

Downloaded from https://www.cambridge.org/core. UNIVERSIDAD AUTONOMA METROPOLITANA, on 14 Nov 2026 at 01:30:40, subject to the Cambridge Core terms of use, available at https://www.cambridge.org/core/terms. https://doi.org/10.1017/CBO9781107706620.010

part – the only possibility that can support the special kinematics $|\hat{i}\rangle \propto |i+1\rangle \propto |\hat{P}_{i,i+1}\rangle$ – and the remainder L-loop integrand:



(7.19)

Note that the lines in this figure are labeled by momentum supertwistors, so we place a hat just on line i since that is the only shifted momentum twistor.

▶ **Exercise 7.4**

Show that for $w \to \infty$, the kinematics give

$$|\widehat{i-1}\rangle = |i-1\rangle\,, \qquad |\widehat{i-1}] = |i-1] - \frac{\langle i, i+1\rangle}{\langle i+1, i-1\rangle}|i]\,,$$
$$|\hat{P}_I\rangle = |i+1\rangle\,, \qquad |\hat{P}_I] = -\left(\frac{\langle i, i-1\rangle}{\langle i+1, i-1\rangle}|i] + |i+1]\right)\,. \tag{7.20}$$

To summarize, BCFW recursion relations in momentum twistor space express the integrand (superamplitude) as a boundary contribution $\mathcal{B}_\infty$ from $w = \infty$ plus a sum of residues at finite w. Schematically, we have

$$\mathcal{I}_n^L = \hat{\mathcal{I}}_n^L(w=0) = \mathcal{B}_\infty^L - \sum_{w_* \neq 0}\left(\text{Residues of } \frac{\hat{\mathcal{I}}_n^L(w)}{w} \text{ at finite } w_*\right)\,. \tag{7.21}$$

The boundary term $\mathcal{B}_\infty$ is computable and is given by the diagram (7.19). The rest of the residues come from diagrams such as (7.13).

To become familiar with how this works in practice, we first apply the recursion relations to tree-level superamplitudes before moving on to loop-integrands in Section 7.4.

7.3 Momentum twistor BCFW at tree-level

In Section 4.5.2, we used the super-BCFW recursion relations to show that the NMHV tree-level superamplitude of $\mathcal{N}=4$ SYM can be written as the MHV superamplitude times a sum of the dual superconformal invariants R_{ijk}; see (4.88). We then rewrote the NMHV formula in terms of momentum twistors in Section 5.4 and found (5.60),

$$\mathcal{A}_n^{\text{NMHV}} = \mathcal{A}_n^{\text{MHV}} \sum_{j=2}^{n-3}\sum_{k=j+2}^{n-1}\big[n, j-1, j, k-1, k\big]\,, \tag{7.22}$$

Downloaded from https://www.cambridge.org/core. UNIVERSIDAD AUTONOMA METROPOLITANA, on 14 Nov 2026 at 01:30:40, subject to the Cambridge Core terms of use, available at https://www.cambridge.org/core/terms. https://doi.org/10.1017/CBO9781107706620.010

where the 5-brackets $[n, j-1, j, k-1, k] \equiv R_{njk}$ are invariant under cyclic permutations of the five labels. It was claimed then that the N^KMHV tree superamplitudes took a similar form but with the sum involving products of K 5-brackets. We now prove this statement using the momentum twistor formulation of super-BCFW. This also serves to prove that the tree superamplitudes of $\mathcal{N}=4$ SYM are dual superconformal covariant.

Adapted to tree-level, the $\hat{Z}_i$-shift BCFW relation (7.21) reads

$$\mathcal{A}_n = \mathcal{B}_\infty - \sum_{j=i-3}^{i+2} \left(\text{Residues of } \frac{\hat{\mathcal{A}}_n(w)}{w} \text{ at } \hat{y}_{ij}^2 = 0 \right) . \tag{7.23}$$

We begin with a detailed evaluation of the boundary term.

The boundary term $\mathcal{B}_\infty$. Per definition, the boundary contribution is the residue of the pole at infinity,[2]

$$\mathcal{B}_\infty = -\oint_{\mathcal{C}_\infty} \frac{dw}{w}\, \hat{\mathcal{A}}_n(w)\,. \tag{7.24}$$

Here $\mathcal{C}_\infty$ is a contour that surrounds $w=\infty$ counterclockwise. Since we are more familiar with the shift in momentum space, let us change variables from w to z. With the help of (7.8) we find

$$\mathcal{B}_\infty = \oint_{\mathcal{C}_{z_*}} dz\, \frac{z_*}{z(z-z_*)}\, \hat{\mathcal{A}}_n(z)\,, \tag{7.25}$$

where $z_* = \frac{\langle i,i+1\rangle}{\langle i-1,i+1\rangle}$ is the value of z at $w=\infty$. Now we need to find out how the shifted n-point amplitude behaves for z near z_*. We have already established in (7.19) that the N^KMHV superamplitude factorizes as $\mathrm{N}^K\mathrm{MHV}_{n-1}\times\text{anti-MHV}_3$ at $z=z_*$. Let us focus on the **MHV case** ($K=0$) first to see explicitly how this comes about. Under the $[i-1,i\rangle$-supershift, the Grassmann delta function in the MHV superamplitude is inert, and the only part of the amplitude affected by the shift is the denominator factor $\langle \hat{i}, i+1\rangle$. This exactly is the factorization pole for $z\to z_*$. Therefore, near z_* we can write

$$\hat{\mathcal{A}}_n^{\mathrm{MHV}}(z) \xrightarrow{z\to z_*} \hat{\mathcal{A}}_{n-1}^{\mathrm{MHV}}(z_*)\, \frac{1}{\hat{P}_I^2}\, \hat{\mathcal{A}}_3^{\text{anti-MHV}}(z_*) = \frac{P_I^2}{\hat{P}_I^2} \left[\hat{\mathcal{A}}_{n-1}^{\mathrm{MHV}}(z_*)\, \frac{1}{P_I^2}\, \hat{\mathcal{A}}_3^{\text{anti-MHV}}(z_*) \right]. \tag{7.26}$$

We know from super-BCFWing the MHV superamplitude in Section 4.5.1 that the factor $[\ldots]$ in (7.26) equals $\mathcal{A}_n^{\mathrm{MHV}}$ (remember, for MHV only one diagram contributed in the recursion relations based on a BCFW shift of adjacent lines). The prefactor is $\frac{P_I^2}{\hat{P}_I^2} = -z_*/(z-z_*)$. Thus

$$\mathcal{B}_\infty^{\mathrm{MHV}} = -\mathcal{A}_n^{\mathrm{MHV}} \oint_{\mathcal{C}_{z_*}} dz\, \frac{z_*^2}{z(z-z_*)^2} = \mathcal{A}_n^{\mathrm{MHV}}\,. \tag{7.27}$$

[2] We ignore the $2\pi i$ of the Cauchy theorem since all such factors drop out at the end.

Downloaded from https://www.cambridge.org/core. UNIVERSIDAD AUTONOMA METROPOLITANA, on 14 Nov 2026 at 01:30:40, subject to the Cambridge Core terms of use, available at https://www.cambridge.org/core/terms. https://doi.org/10.1017/CBO9781107706620.010

In the second equality, we evaluated the double pole integral using

$$\oint dz\, \frac{f(z)}{(z-z_*)^2} = \frac{d}{dz_*} \oint dz\, \frac{f(z)}{(z-z_*)} = f'(z_*) \tag{7.28}$$

for the case $f(z) = 1/z$.

What we have achieved for the MHV case here is a verification of the simple statement that the MHV tree-level superamplitude satisfies the super-BCFW recursion relations, which for MHV include only one term, namely the $\text{MHV}_{n-1} \times \text{anti-MHV}_3$ diagram. We knew that already more than 50 pages ago (Section 4.5.1), but the point is that here we have set up the calculation in a way that facilitates the generalization to N^KMHV level. And that is what we do next.

N^KMHV case. Assume inductively that the $(n-1)$-point tree-level N^KMHV superamplitude can be written as an MHV prefactor times a function we will call $Y_{n-1}^{(K)}$. We know that $Y_n^{(0)} = 1$ and that $Y_n^{(1)}$ is the sum of 5-brackets given in (7.22). In particular, $Y_n^{(0)}$ and $Y_n^{(1)}$ are dual superconformal invariants. The aim here will be to use BCFW to derive a recursive expression for $Y_n^{(K)}$ in terms of Ys with smaller K and n. This will prove that $Y_n^{(K)}$ is a dual superconformal invariant for all n and k.

The calculation of the contribution from $w = \infty$ follows the same steps as the MHV case, except that the factorization (7.26) is now replaced by

$$\hat{\mathcal{A}}_n^{\text{MHV}}(z) \xrightarrow{z \to z_*} \hat{\mathcal{A}}_{n-1}^{\text{MHV}}(z_*)\, \widehat{Y}_{n-1}^{(K)}(z_*)\, \frac{1}{\hat{P}_I^2}\, \hat{\mathcal{A}}_3^{\text{anti-MHV}}(z_*)\,. \tag{7.29}$$

Let us take a closer look at the Y-factor. It is naturally a function of momentum supertwistors

$$\widehat{Y}_{n-1}^{(K)}(z_*) \;=\; \widehat{Y}_{n-1}^{(K)}(\ldots, \mathcal{Z}_{i-1}, \mathcal{Z}_I, \mathcal{Z}_{i+2}, \ldots)\,. \tag{7.30}$$

Now in our analysis of the kinematics, we learned that the momentum twistor $\mathcal{Z}_I$ is characterized as the intersection (7.16) between the line $(j-1, j)$ and the plane $(i-1, i, i+1)$. In our case here, we have $j = i+2$, so (7.16) says that $\mathcal{Z}_I$ is the point of intersection between the line $(i+1, i+2)$ and the plane $(i-1, i, i+1)$. Obviously this intersection point is $\mathcal{Z}_{i+1}$, i.e.

$$\text{For } w = \infty \text{ case:} \quad (I) = (i+1, i+2) \bigcap (i-1, i, i+1) = (i+1)\,. \tag{7.31}$$

So we can freely substitute $\mathcal{Z}_I \to \mathcal{Z}_{i+1}$ to find

$$\widehat{Y}_{n-1}^{(K)}(z_*) \;=\; Y_{n-1}^{(K)}(\ldots, \mathcal{Z}_{i-1}, \mathcal{Z}_{i+1}, \mathcal{Z}_{i+2}, \ldots)\,. \tag{7.32}$$

This factor is independent of z and we can therefore repeat our argument from the MHV case to find

$$\mathcal{B}_\infty^{\text{N}^K\text{MHV}} = \oint_{\mathcal{C}_\infty} \frac{dw}{w}\, \hat{\mathcal{A}}_n^{\text{N}^K\text{MHV}}(w) = \mathcal{A}_n^{\text{MHV}}\; Y_{n-1}^{(K)}(\mathcal{Z}_1, \ldots, \mathcal{Z}_{i-1}, \mathcal{Z}_{i+1}, \ldots \mathcal{Z}_n)\,. \tag{7.33}$$

This completes the calculation of the boundary term.

Residues at finite w. Now we extract the residues of the finite poles in the w-plane. They arise from propagators $1/\hat{y}_{ij}^2$ going on-shell. Writing the shifted propagator in terms of

Downloaded from https://www.cambridge.org/core. UNIVERSIDAD AUTONOMA METROPOLITANA, on 14 Nov 2026 at 01:30:40, subject to the Cambridge Core terms of use, available at https://www.cambridge.org/core/terms. https://doi.org/10.1017/CBO9781107706620.010

momentum twistor, we find

$$\frac{1}{\hat{y}_{ij}^2} = \frac{\langle \hat{i}, i-1\rangle\langle j, j-1\rangle}{\langle \hat{i}, i-1, j, j-1\rangle} = \frac{\langle i, i-1\rangle\langle j, j-1\rangle}{\langle i, i-1, j, j-1\rangle + w\langle i+1, i-1, j, j-1\rangle} = \frac{w_*}{y_{ij}^2}\frac{1}{w-w_*}, \tag{7.34}$$

where $w_* = -\frac{\langle i,i-1,j,j-1\rangle}{\langle i+1,i-1,j,j-1\rangle}$. This means that

$$-\int_{\mathcal{C}(w_*)} \frac{dw}{w}\frac{1}{\hat{y}_{ij}^2} f(w) = -\int_{\mathcal{C}(w_*)} \frac{dw}{w}\frac{w_*}{y_{ij}^2}\frac{1}{w-w_*} f(w) = \frac{1}{y_{ij}^2} f(w_*). \tag{7.35}$$

So the contribution from the shifted propagator is simply the unshifted propagator, exactly the same as the usual BCFW rules. In a given factorization channel, we can write the left and the right subamplitudes as:

$$\begin{aligned} \mathcal{A}_{n_L} &= \mathcal{A}_{n_L}^{\text{MHV}}\, Y_{n_L}^{(K_L)}(\mathcal{Z}_I, \mathcal{Z}_{j-1}, \ldots, \mathcal{Z}_{i+1}, \mathcal{Z}_{\hat{i}}), \\ \mathcal{A}_{n_R} &= \mathcal{A}_{n_R}^{\text{MHV}}\, Y_{n_R}^{(K_R)}(\mathcal{Z}_I, \mathcal{Z}_{i-1}, \ldots, \mathcal{Z}_{j+1}, \mathcal{Z}_j). \end{aligned} \tag{7.36}$$

Here the Grassmann degrees obey $K_R + K_L + 1 = K$; in particular this is why there were no such diagrams for the MHV case. The contribution of the BCFW channel is simply

$$\left(\sum_{\text{states}} \frac{\hat{\mathcal{A}}_{n_L}^{\text{MHV}}\,\hat{\mathcal{A}}_{n_R}^{\text{MHV}}}{P_I^2}\right) \widehat{Y}_{n_L}^{(K_L)}(\mathcal{Z}_I, \mathcal{Z}_{j-1}, \ldots, \mathcal{Z}_{i+1}, \hat{\mathcal{Z}}_i)\, \widehat{Y}_{n_R}^{(K_R)}(\mathcal{Z}_I, \mathcal{Z}_{i-1}, \ldots, \mathcal{Z}_{j+1}, \mathcal{Z}_j). \tag{7.37}$$

The $\mathcal{Z}_I$ appearing in the dual superconformal invariants $Y_{\text{L,R}}$ can be written in terms of the external line supermomentum twistors using the characterization of $\mathcal{Z}_I$ as an intersection point (7.16) and the formula (5.66), similarly for $\hat{\mathcal{Z}}_i$, via the intersection rule (7.15).

As a consequence, the state sum – which is an integration over the η_I variables – acts solely on the MHV prefactors. Furthermore, the factor in parenthesis is in (7.37) simply the BCFW term of the NMHV amplitude arising from the P_I factorization channel. We have calculated this in Section 4.5.2, and later learned that in the momentum twistor language the answer is written in terms of the 5-bracket:

$$\left(\sum_{\text{states}} \frac{\hat{\mathcal{A}}_{n_L}^{\text{MHV}}\,\hat{\mathcal{A}}_{n_R}^{\text{MHV}}}{P_I^2}\right) = \mathcal{A}_n^{\text{MHV}}\big[i-1, i, i+1, j-1, j\big]. \tag{7.38}$$

Thus we have finally arrived at the BCFW recursion relation for tree-level amplitudes in $\mathcal{N}=4$ SYM, written in momentum twistor space:

$$\mathcal{A}_n^{\text{N}^K\text{MHV}} = \mathcal{A}_n^{\text{MHV}}\Bigg\{ Y_{n-1}^{(K)}(\ldots, \mathcal{Z}_{i-1}, \mathcal{Z}_{i+1}, \mathcal{Z}_{i+2}, \ldots) + \sum_{j=i+3}^{i-2} \big[i-1, i, i+1, j-1, j\big] \times \widehat{Y}_{n_L}^{(K_L)}(\mathcal{Z}_I, \mathcal{Z}_j, \mathcal{Z}_{j+1}, \ldots, \mathcal{Z}_{i-1}) \times \widehat{Y}_{n_R}^{(K_R)}(\mathcal{Z}_I, \hat{\mathcal{Z}}_i, \mathcal{Z}_{i+1}, \ldots, \mathcal{Z}_{j-1}) \Bigg\}. \tag{7.39}$$

Downloaded from https://www.cambridge.org/core. UNIVERSIDAD AUTONOMA METROPOLITANA, on 14 Nov 2026 at 01:30:40, subject to the Cambridge Core terms of use, available at https://www.cambridge.org/core/terms. https://doi.org/10.1017/CBO9781107706620.010

The above relation corresponds to the shift defined in (7.5), and the momentum twistors $\hat{\mathcal{Z}}_i$ and $\mathcal{Z}_I$ are given by (7.15) and (7.16) respectively. Also, there are implicit sums over $K_R + K_L + 1 = K$ and $n_L + n_R = n + 2$.

▶ **Exercise 7.5**

Show that (7.39) gives the known NMHV expression (7.22) for $K = 1$.

The result (7.39) verifies the claim that all tree-level amplitudes of $\mathcal{N} = 4$ SYM can be written as an MHV prefactor times polynomials of 5-brackets: given that this is true for the NMHV amplitudes, (7.39) ensures that the 5-brackets are recycled into the higher-K results. Since the 5-brackets are manifestly dual superconformal invariant, so are all tree-level superamplitudes of $\mathcal{N} = 4$ SYM.

7.4 Momentum twistor BCFW for planar loop-integrands

To initiate the discussion of BCFW recursion for planar loop-integrands of $\mathcal{N} = 4$ SYM, let us examine a specific example to get some intuition for the good looks and behaviors of integrands. In other words, we start with the answer and let that guide our discussion.

In Section 6.2, we used the generalized unitarity method to construct the 1-loop $\mathcal{N} = 4$ SYM superamplitude. We found

$$\mathcal{A}_4^{\text{1-loop}}[1234] = su\, \mathcal{A}_4^{\text{tree}}[1234]\, I_4(p_1, p_2, p_3, p_4)\,, \tag{7.40}$$

where I_4 is the 1-loop box-integral which we wrote in dual y-space in (7.4) as

$$I_4(p_1, p_2, p_3, p_4) = \int \frac{d^4 y_0}{y_{01}^2\, y_{02}^2\, y_{03}^2\, y_{04}^2}\,. \tag{7.41}$$

Here the propagator-terms $y_{0i}^2 = (y_0 - y_i)^2$ involve the zone-variable y_0 associated with the loop-momentum, as indicated in (7.3).

The expressions (7.40), (7.41) determine the loop-integrand for the 4-point 1-loop $\mathcal{N} = 4$ SYM superamplitude to be (using $-s = y_{13}^2$ and $-u = y_{24}^2$)

$$\mathcal{I}_4^{\text{1-loop}}[1234] = \mathcal{A}_4^{\text{tree}}[1234]\, \frac{y_{13}^2\, y_{24}^2}{y_{01}^2\, y_{02}^2\, y_{03}^2\, y_{04}^2}\,. \tag{7.42}$$

Now, to translate this to momentum twistor space, recall that a point y in dual space maps to a line in momentum twistor space. So let us take y_0 to be mapped to some line (A, B) determined by two points $\mathcal{Z}_A$ and $\mathcal{Z}_B$; then the loop-integral $\int d^4 y_0$ maps to an integral over all inequivalent lines (A, B). There is a story here of how to define the integration measure appropriately – we postpone this until later in this section in order to first discuss the structure of the loop-integrands.

Downloaded from https://www.cambridge.org/core. UNIVERSIDAD AUTONOMA METROPOLITANA, on 14 Nov 2026 at 01:30:40, subject to the Cambridge Core terms of use, available at https://www.cambridge.org/core/terms. https://doi.org/10.1017/CBO9781107706620.010

Using (5.52) to rewrite all the dual variables y in the integrand in terms of 4-brackets, in particular $y_{0i}^2 = \frac{\langle A,B,i-1,i\rangle}{\langle AB\rangle\langle i-1,i\rangle}$, we arrive at the expression

$$\mathcal{I}_4^{\text{1-loop}}[1234] = -\mathcal{A}_4^{\text{tree}}[1234]\,\frac{\langle 1234\rangle^2\langle AB\rangle^4}{\langle AB12\rangle\langle AB23\rangle\langle AB34\rangle\langle AB41\rangle}\,. \tag{7.43}$$

Note that all $\langle i-1,i\rangle$s dropped out. The factor $\langle AB\rangle^4$ will eventually be absorbed in the integration measure and what remains is manifestly dual conformal invariant.

The expression (7.43) is an example of what a 1-loop integrand looks like in momentum twistor space. Under a super-BCFW shift $\hat{\mathcal{Z}}_4 = \mathcal{Z}_4 + w\mathcal{Z}_3$, the integrand has a pole that involves the loop-momentum: it comes from $\langle AB\hat{4}1\rangle = 0$. The residue of such a pole is the new input we need for the loop-level recursion relations.

▶ **Exercise 7.6**

What type of super-BCFW shift is induced in momentum space by the momentum twistor shift $\hat{\mathcal{Z}}_4 = \mathcal{Z}_4 + w\mathcal{Z}_3$?

Next, we outline the form of the recursion relations for general L-loop integrands.

Structure of the BCFW recursion for loop-integrands

Without loss of generality, we consider the recursion relations derived from a shift of the nth momentum twistor,

$$\hat{\mathcal{Z}}_n = \mathcal{Z}_n + w\mathcal{Z}_{n-1}\,. \tag{7.44}$$

For an n-point L-loop integrand, there will be three distinct types of contributions to the recursion relations:

1. The boundary contribution from $w \to \infty$. This contribution is calculated just as in the tree-level case of the previous section, so we simply state the result (suppressing the K of the N^KMHV classification)

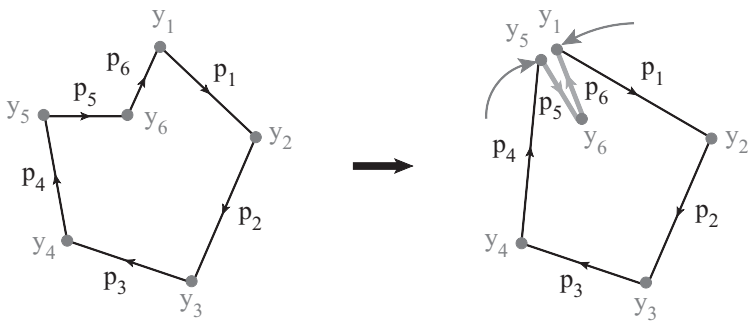
$$\text{term at } w\to\infty: \qquad \mathcal{A}^{\text{tree}}_{n,\text{MHV}}\, Y^L_{n-1}\big(\mathcal{Z}_1,\ldots,\mathcal{Z}_{n-1}\big)\,. \tag{7.45}$$

   Here Y^L_{n-1} is, by the inductive assumption, an L-loop dual superconformal invariant.
2. Residues of factorization channels from propagators that do *not* involve loop-momenta correspond to poles in $\hat{y}^2_{1j} \propto \langle \hat{n}, 1, j-1, j\rangle = 0$. The results for these also follow the same steps as the tree-level case, and one finds

$$\mathcal{A}^{\text{tree}}_{n,\text{MHV}} \sum_{j=3}^{n-2} \big[j-1, j, n-1, n, 1\big]\, Y_{\text{L}}^{L_1}\big(\mathcal{Z}_{I_j}, \mathcal{Z}_j, \mathcal{Z}_{j+1},\ldots,\hat{\mathcal{Z}}_{n_j}\big)\, Y_{\text{R}}^{L_2} \times \big(\mathcal{Z}_{I_j}, \mathcal{Z}_1, \mathcal{Z}_2,\ldots,\mathcal{Z}_{j-1}\big)\,, \tag{7.46}$$

   where $\hat{\mathcal{Z}}_{n_j} = (n-1,n)\bigcap(1,j-1,j)$ and $\mathcal{Z}_{I_j} = (j,j-1)\bigcap(n-1,n,1)$. This includes an implicit sum over loop-orders L_1 and L_2 in the sub-integrands such that $L_1 + L_2 = L$. Also, the N^KMHV level was suppressed, and one must sum over the Grassmann degrees associated with the sub-integrands such that $K_{\text{L}} + K_{\text{R}} = K - 1$.

Downloaded from https://www.cambridge.org/core. UNIVERSIDAD AUTONOMA METROPOLITANA, on 14 Nov 2026 at 01:30:40, subject to the Cambridge Core terms of use, available at https://www.cambridge.org/core/terms. https://doi.org/10.1017/CBO9781107706620.010



The forward limit illustrated in dual coordinates. The limit corresponds to y_5 and y_1 approaching a point while satisfying $y_{14}^2 = 0$. Fig. 7.4

3. Residues of factorization channels from propagators that *do* involve loop-momenta; they correspond to

$$\langle A\, B\, \hat{n}\, 1\rangle = 0\,. \tag{7.47}$$

These are the new forward limit contributions at loop-level, so we will take a closer look at them now.

Forward limit contributions

For an L-loop n-point integrand, the residue of the pole (7.47) is an $(L-1)$-loop $(n+2)$-point integrand whose two extra legs are evaluated in the forward limit (7.1), as shown in Figure 7.1. The following example of $n = 4$ will illustrate the idea of how to do this.

▷ *Example.* Start with a 6-point $(L-1)$-loop integrand. Translated to dual coordinates, the forward limit of p_5 and p_6 approaching $p_5 = -p_6 = r$ is the limit of taking $y_1 \to y_5$ while y_6 remains fixed. This is illustrated in Figure 7.4. In momentum twistor space, the point y_1 is determined by the line $(1, 6)$ and y_5 by $(4, 5)$, so y_1 and y_5 can be identified only when (Z_1, Z_6, Z_5, Z_4) lie on the same line. It is easy to achieve this configuration if the line $(1, 4)$ intersects line $(6, 5)$, because then we can send Z_5 and Z_6 to the intersection point $(6, 5)\bigcap(1, 4)$. Note that this does not change y_6, but the result is $y_1 \to y_5$.

However, momentum twistors live in $\mathbb{CP}^3$ where two lines generically do not intersect. So we cannot take the limit as naively as above. Instead, we modify the momentum twistor $Z_4 \to \hat{Z}_4 = Z_4 + wZ_3$, and tune w such that the new line $(1, \hat{4})$ intersects $(5, 6)$: let $Z_{\hat{B}}$ be the point of intersection. Since $\hat{Z}_4$ per construction lies on the line $(3, 4)$, we can characterize $Z_{\hat{B}}$ as the intersection point between the line $(5, 6)$ and the plane $(3, 4, 1)$ (see Figure 7.5):

$$Z_{\hat{B}} = (5, 6)\bigcap(3, 4, 1)\,. \tag{7.48}$$

Because the lines $(1, \hat{4})$ and $(5, 6)$ are arranged to intersect, it follows that $\hat{Z}_4$ lies in the plane $(5, 6, 1)$, see Figure 7.5. But $\hat{Z}_4$ is also on the line $(3, 4)$, so the shifted

Downloaded from https://www.cambridge.org/core. UNIVERSIDAD AUTONOMA METROPOLITANA, on 14 Nov 2026 at 01:30:40, subject to the Cambridge Core terms of use, available at https://www.cambridge.org/core/terms. https://doi.org/10.1017/CBO9781107706620.010

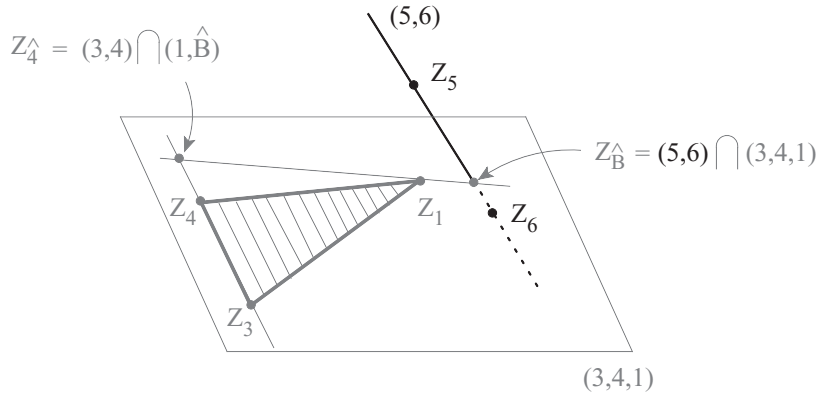


Fig. 7.5 The geometry of the forward limit Figure 7.4 illustrated here in momentum twistor space. The point $Z_{\hat{B}}$ is defined as the intersection of line (Z_5, Z_6) with plane (Z_1, Z_3, Z_4). The BCFW-deformed $\hat{Z}_4$ is fixed at the interaction of line (Z_3, Z_4) and $(Z_{\hat{B}}, Z_1)$. The gray points lie in the same plane.

momentum twistor can be identified in terms of the unshifted lines as

$$\hat{Z}_4 = (3,4)\bigcap(5,6,1)\,. \tag{7.49}$$

The setup with (7.48) and (7.49) allows us to take the forward limit directly by sending Z_5, Z_6 to the intersection point $Z_{\hat{B}}$. We can summarize the deformation and forward limit $p_5 = -p_6 = r$ as

$$(Z_1, Z_2, Z_3, Z_4, Z_5, Z_6) \to (Z_1, Z_2, Z_3, \hat{Z}_4, Z_5, Z_6)\Big|_{Z_5, Z_6 \to Z_{\hat{B}}}\,. \tag{7.50}$$

It is important to note that $\hat{Z}_4$ satisfies

$$\langle 5, 6, \hat{4}, 1\rangle = 0\,. \tag{7.51}$$

Comparing (7.51) with (7.47), we recognize the single-cut condition (or equivalently, momentum dependent pole in BCFW) provided that Z_5 and Z_6 are identified as the loop-momentum twistors Z_A and Z_B. This is also the statement that y_6 has been identified as the Lth loop integration region, as Figure 7.4 indicates that it should be. ◁

Let us return to the general case. The forward limit is taken for $(L-1)$-loop $(n+2)$-point integrands by sending the momentum twistors $(\hat{Z}_n, Z_A, Z_B)$ to the forward configuration discussed in the example. One must multiply by an overall MHV factor as well as the result for the cut propagator. The result (which we discuss further below) is

$$\mathcal{A}^{\text{tree}}_{n,\text{MHV}} \times f(A, B, n-1, n, 1) \times \left(Y^{L-1}_{n+2}[\mathcal{Z}_1, \mathcal{Z}_2, \ldots, \hat{\mathcal{Z}}_{n_{AB}}, \mathcal{Z}_A, \mathcal{Z}_B]\Big|_{A,B\to\hat{B}} \right), \tag{7.52}$$

where adapting (7.48) and (7.49) to the n-point case with $5 \to A$ and $6 \to B$ identifies

$$\hat{\mathcal{Z}}_{n_{AB}} = (n-1, n)\bigcap(A, B, 1) \quad \text{and} \quad \hat{B} = (A, B)\bigcap(n-1, n, 1)\,. \tag{7.53}$$

Downloaded from https://www.cambridge.org/core. UNIVERSIDAD AUTONOMA METROPOLITANA, on 14 Nov 2026 at 01:30:40, subject to the Cambridge Core terms of use, available at https://www.cambridge.org/core/terms. https://doi.org/10.1017/CBO9781107706620.010

Here, $f(A, B, n-1, n, 1)$ represents the kinematic function which includes the cut propagator as well as possible Jacobian factors that arise from solving the single cut constraint, $\langle A, B, \hat{n}, 1\rangle = 0$. We will determine this function shortly, but first we address one important missing piece: what to do about the Z_A and Z_B momentum twistors and how the extra loop-momenta integral emerges from the forward limit. That is the next step.

The integration measure

The forward limit is taken of a higher point amplitude/integrand, so we need to devise a way to remove the information of the two extra external legs. The most naive proposal is to apply the following integration:

$$\int d^{4|4}\mathcal{Z}_A d^{4|4}\mathcal{Z}_B \,. \tag{7.54}$$

Surprisingly, this is essentially the correct answer! The reason it is correct is rather non-trivial. Let us first consider the bosonic part of the integration. The integration over Z_A and Z_B can be decomposed into two pieces, one is the integration over all possible lines (A, B), and the other is the movement of Z_A and Z_B along a particular line (A, B). To aid this separation, consider the following $GL(2)$ transformation on (Z_A, Z_B),

$$\begin{pmatrix} Z_{A'} \\ Z_{B'} \end{pmatrix} = \begin{pmatrix} c_{A'}{}^{A} & c_{A'}{}^{B} \\ c_{B'}{}^{A} & c_{B'}{}^{B} \end{pmatrix} \begin{pmatrix} Z_A \\ Z_B \end{pmatrix}. \tag{7.55}$$

The above 2×2 matrix exactly parameterizes the movement along the line (A, B), because the new pair (A', B') defines the same line as (A, B). In the forward limit, we are sending Z_A and Z_B on a given line to the intersection of (A, B) with the plane $(n-1, n, 1)$, so this limit corresponds to a particular solution for the $GL(2)$ matrix. In light of this, it will be convenient to separate the bosonic integral as

$$\int d^4 Z_A d^4 Z_B = \int \frac{d^4 Z_A d^4 Z_B}{\mathrm{Vol}[GL(2)]} \int_{GL(2)} . \tag{7.56}$$

The $\mathrm{Vol}[GL(2)]$ in the denominator indicates that as one integrates over the 4×2 dimensional space of Z_A and Z_B, one needs to mod out the 2×2 c-matrix in (7.55) that parameterizes an arbitrary $GL(2)$ transformation. The explicit integration measure for $\int_{GL(2)}$ can be fixed by requiring it to be $SL(2)$ invariant and having $GL(1)$ weight 4 in both A and B.[3] This fixes the form to be

$$\int_{GL(2)} = \int \langle c_{A'} dc_{A'}\rangle \langle c_{B'} dc_{B'}\rangle \langle c_{A'} c_{B'}\rangle^2 \,, \tag{7.57}$$

where $\langle c_{A'} c_{B'}\rangle = c_{A'}{}^{A} c_{B'}{}^{B} - c_{A'}{}^{B} c_{B'}{}^{A}$. After one has separated out the $GL(2)$ integral, the remaining integration measure can be naturally related to the y_0 measure. To see this, note that after stripping off the $GL(2)$ part, the remaining measure is purely integrating over all distinct lines (A, B). Recall that distinct lines in twistor space define distinct points in dual space, so this tells us that this measure is precisely proportional to $\int d^4 y_0$. The precise

[3] This follows from the fact that there are four-components in Z_A and Z_B.

Downloaded from https://www.cambridge.org/core. UNIVERSIDAD AUTONOMA METROPOLITANA, on 14 Nov 2026 at 01:30:40, subject to the Cambridge Core terms of use, available at https://www.cambridge.org/core/terms. https://doi.org/10.1017/CBO9781107706620.010

momentum twistor integral that is equivalent to the loop-integral over y_0 is

$$\int d^4 y_0 = \int \frac{d^4 Z_A d^4 Z_B}{\text{Vol}[GL(2)]\langle AB\rangle^4}\,, \tag{7.58}$$

where the four extra factors of $\langle AB\rangle$ in the denominator are necessary for the measure to be projective. The angle bracket $\langle AB\rangle$ breaks the $SL(4)$ invariance because it picks only the angle spinor piece of the momentum twistors. This breaks dual conformal invariance – but that is expected because the $d^4 y_0$ inverts non-trivially under dual conformal inversion. From our example (7.43), we see that the $\langle AB\rangle^4$-factor in the measure is exactly canceled by the $\langle AB\rangle^4$-factor that appeared when we rewrote the box-integral in momentum twistor space. This is a general feature which follows from (or, if you prefer, is necessary for) the dual conformal invariance of the loop-integrand. Henceforth, we simply implicitly assume the cancellation of the $\langle AB\rangle^4$s. Let us for later reference write what the 1-loop 4-point superamplitude looks like when dressed in full momentum twistor regalia:

$$\mathcal{A}_4^{\text{1-loop}}[1234] = -\mathcal{A}_4^{\text{tree}}[1234] \int \frac{d^4 Z_A d^4 Z_B}{\text{Vol}[GL(2)]} \frac{\langle 1234\rangle^2}{\langle AB12\rangle\langle AB23\rangle\langle AB34\rangle\langle AB41\rangle}\,. \tag{7.59}$$

Back to the forward-limit discussion. To integrate over all possible configurations of the forward limit, one should only integrate over all distinct lines (A, B). This requires us to remove the $GL(2)$-part of the integration in (7.54). Thus we have two problems to solve, how to put the higher-point amplitude on the forward limit and how to remove the $GL(2)$ redundancy. Fortunately, we can scare two birds with one stone![4] We begin by simply presenting the resolution: the correct prescription for the computation of the forward limit is

$$\mathcal{A}^{\text{tree}}_{n,\text{MHV}} \int \frac{d^{4|4}\mathcal{Z}_A d^{4|4}\mathcal{Z}_B}{\text{Vol}[GL(2)]} \int_{\text{GL(2)}} [A, B, n-1, n, 1] \times Y^{L-1}_{n+2}[\mathcal{Z}_1, \mathcal{Z}_2, \ldots, \hat{\mathcal{Z}}_{n_{AB}}, \mathcal{Z}_A, \mathcal{Z}_{\hat{B}}]\,, \tag{7.60}$$

where $\mathcal{Z}_B$ is sent to the intersection $\hat{B} = (A, B)\bigcap(n-1, n, 1)$. Note the appearance of the factor $[A, B, n-1, n, 1]$. The role this factor plays is two-fold:

- It contains the invariants $\langle A, n-1, n, 1\rangle$ and $\langle B, n-1, n, 1\rangle$ in the denominator. The vanishing of these invariants is precisely the forward limit, and therefore these poles can be used to localize the $GL(2)$ integral on to the forward limit. (The two birds fly away.)
- It also contains the factor $1/\langle A, B, n, 1\rangle$, which is precisely the single-cut propagator.

Hence the $GL(2)$ integration is understood to encircle poles that correspond to the forward limit. One may ask if $[A, B, n-1, n, 1]$ is the unique function that satisfies the above two points. The answer is no, however, it can be easily justified by dual conformal invariance. The recursion better preserves this symmetry. With Y^{L-1}_{n+2} already an invariant, $[A, B, n-1, n, 1]$ is the unique invariant that satisfies the above two properties. Thus, using

[4] No need for excessive aggression.

Downloaded from https://www.cambridge.org/core. UNIVERSIDAD AUTONOMA METROPOLITANA, on 14 Nov 2026 at 01:30:40, subject to the Cambridge Core terms of use, available at https://www.cambridge.org/core/terms. https://doi.org/10.1017/CBO9781107706620.010

symmetry arguments we did not need to know a priori what the function $f(A, B, n-1, n, 1)$ in (7.52) should be; it is whatever $[A, B, n-1, n, 1]$ evaluates to once the $GL(2)$ integral is localized. This is admittedly rather abstract, but we are going to realize the contents of the discussion here explicitly when we compute the 4-point 1-loop amplitude in Section 7.5.

Finally, we need to sum over all $\mathcal{N}=4$ SYM states that can run in the forward limit loop. In (7.60) this is naturally achieved in a way that preserves the dual superconformal symmetry by simply extending the bosonic momentum twistor integration to include the Grassmann-components, χ_A and χ_B. We are now ready to put everything together.

Result of the BCFW recursion for L-loop integrands

Summarizing the preceding discussion, the loop-level BCFW recursion relation is given by

$$\begin{aligned}
&\mathcal{A}_n^{L\text{-loop}} \\
&= \mathcal{A}^{\text{tree}}_{n,\text{MHV}} \Bigg\{ Y^L_{n-1}\big(\mathcal{Z}_1, \ldots, \mathcal{Z}_{n-1}\big) \\
&\quad + \sum_{j=3}^{n-2} \big[j-1, j, n-1, n, 1\big] Y_{\text{L}}^{L_1}\big(\mathcal{Z}_{I_j}, \mathcal{Z}_j, \mathcal{Z}_{j+1}, \ldots, \hat{\mathcal{Z}}_{n_j}\big) Y_{\text{R}}^{L_2}\big(\mathcal{Z}_{I_j}, \mathcal{Z}_1, \mathcal{Z}_2, \ldots, \mathcal{Z}_{j-1}\big) \\
&\quad + \int \frac{d^{4|4}\mathcal{Z}_A d^{4|4}\mathcal{Z}_B}{\text{Vol}[GL(2)]} \int_{GL(2)} [A, B, n-1, n, 1]\; Y^{L-1}_{n+2}[\mathcal{Z}_1, \mathcal{Z}_2, \ldots, \hat{\mathcal{Z}}_{n_{AB}}, \mathcal{Z}_A, \mathcal{Z}_{\hat{B}}] \Bigg\}.
\end{aligned} \tag{7.61}$$

In the second line, L_1 and L_2 are summed over subject to $L_1 + L_2 = L$, as are the Grassmann degrees $K_1 + K_2 = K - 1$, and we have

$$\begin{aligned}
\hat{\mathcal{Z}}_{n_j} &= (n-1, n) \bigcap (1, j-1, j), \quad \mathcal{Z}_{I_j} = (j, j-1) \bigcap (n-1, n, 1), \\
\hat{\mathcal{Z}}_{n_{AB}} &= (n-1, n) \bigcap (A, B, 1).
\end{aligned} \tag{7.62}$$

In the last line of (7.61), the Grassmann degree of Y^{L-1}_{n+2} is $4(K+1)$, i.e. one level higher than the amplitude on the LHS of the equation.

Before moving on to an explicit application of the loop-integrand recursion relations, it is important to note that (7.61) provides us with the tool to prove dual conformal properties of loop-integrals, just as we did for the tree-level recursion. Assuming the n-point $L' < L$-loop as well as the $(n+2)$-point $(L-1)$-loop integral is given by an MHV tree amplitude times a dual conformal invariant function, then – through (7.61) – the n-point L-loop amplitude will have the same property.

We will now apply the recursion relations developed in this section to show how the 4-point 1-loop integrand (7.43), can be derived recursively from the recursion relation with the input of just a tree amplitude. Sharpen your pencils and keep your eraser close at hand.

Downloaded from https://www.cambridge.org/core. UNIVERSIDAD AUTONOMA METROPOLITANA, on 14 Nov 2026 at 01:30:40, subject to the Cambridge Core terms of use, available at https://www.cambridge.org/core/terms. https://doi.org/10.1017/CBO9781107706620.010

7.5 Example: 4-point 1-loop amplitude from recursion

The 4-point 1-loop amplitude is the simplest example that can illustrate all the novelties of the loop-recursion. Let us examine the potential terms in the recursion formula (7.61):

The *first term* with $Y_3^{L=1}$ is absent. This is because there are no 3-point 1-loop amplitudes. Another way to understand this is that this contribution came from the pole at $w \to \infty$. If we sneak-peak at the answer for the 4-point 1-loop amplitude (7.43), we realize that while the shifted MHV prefactor does have a $w \to \infty$ pole (as we saw and used in Section 7.3), its residue is actually zero for the 1-loop integrand because the $1/\langle AB\hat{4}1\rangle \to 0$ as $w \to \infty$. In other words, we have a consistent picture for the absence of the first term $Y_3^{L=1}$ in (7.61).

The *second term* in (7.61) is absent, again because $Y_3^{L=1} = 0$. This is consistent with (7.43) not having any momentum-independent poles at finite w.

The *third term* in (7.61) is

$$\mathcal{A}_4^{\text{1-loop}} = \mathcal{A}_{4,\text{MHV}}^{\text{tree}} \int \frac{d^{4|4}\mathcal{Z}_A d^{4|4}\mathcal{Z}_B}{\text{Vol}[GL(2)]} \int_{GL(2)} [A, B, 3, 4, 1] \times Y_6[\mathcal{Z}_1, \mathcal{Z}_2, \mathcal{Z}_3, \hat{\mathcal{Z}}_{4_{AB}}, \mathcal{Z}_A, \mathcal{Z}_{\hat{B}}]\,. \tag{7.63}$$

Unfortunately, we now have to evaluate this thing!!

Y_6 is the tree-level NMHV dual conformal invariant for $n = 6$, discussed previously in (5.60):

$$Y_6[\mathcal{Z}_1, \mathcal{Z}_2, \mathcal{Z}_3, \hat{\mathcal{Z}}_{4_{AB}}, \mathcal{Z}_A, \mathcal{Z}_{\hat{B}}] = [\hat{B}, 1, 2, 3, \hat{4}] + [\hat{B}, 1, 2, \hat{4}, A] + [\hat{B}, 2, 3, \hat{4}, A]\,. \tag{7.64}$$

The hatted momentum twistors can be found explicitly using the intersection formulas (5.66). Since the twistors are defined projectively, one can freely include a scaling-factor:

$$(\hat{4}) = (3,4)\bigcap(A, B, 1) \implies \mathcal{Z}_{\hat{4}} = \frac{1}{\langle 3AB1\rangle}\big(\mathcal{Z}_4\langle 3AB1\rangle - \mathcal{Z}_3\langle 4AB1\rangle\big)\,, \tag{7.65}$$

$$(\hat{B}) = (A, B)\bigcap(3, 4, 1) \implies \mathcal{Z}_{\hat{B}} = \frac{1}{\langle A341\rangle}\big(-\mathcal{Z}_A\langle B341\rangle + \mathcal{Z}_B\langle A341\rangle\big)\,. \tag{7.66}$$

For convenience, we pick overall factors such that the "hatted" twistors have the same projective weights as the un-hatted ones. Note that some 4-brackets remain unshifted: $\langle 3, \hat{4}, .., .\rangle = \langle 3, 4, .., .\rangle$ and $\langle A, \hat{B}, .., .\rangle = \langle A, B, .., .\rangle$.

Let us first do the fermionic integrals in $d^{4|4}\mathcal{Z}_A d^{4|4}\mathcal{Z}_B$, i.e. $d^4\chi_A d^4\chi_B$. We have to saturate the Grassmann integrals, so it is only relevant to look at the χ_A- and χ_B-terms in the Grassmann delta functions. Begin with the 5-bracket $[A, B, 3, 4, 1]$ that multiplies each of the three terms in Y_6. Its Grassmann delta function involves

$$[A, B, 3, 4, 1] \;\propto\; \delta^{(4)}\big(\chi_A\langle B341\rangle - \chi_B\langle A341\rangle + \cdots\big)\,. \tag{7.67}$$

It follows from (7.66) that $\chi_{\hat{B}} \propto \chi_A\langle B341\rangle - \chi_B\langle A341\rangle$, so any appearance of $\chi_{\hat{B}}$ in the three 5-brackets in (7.64) vanishes on the support of the $\delta^{(4)}$ in (7.67) under the $\int d^4\chi_A d^4\chi_B$-integral. In particular, the only contribution from χ_A, χ_B in $[\hat{B}, 1, 2, 3, \hat{4}]$ is through $\chi_{\hat{B}}$, so

Downloaded from https://www.cambridge.org/core. UNIVERSIDAD AUTONOMA METROPOLITANA, on 14 Nov 2026 at 01:30:40, subject to the Cambridge Core terms of use, available at https://www.cambridge.org/core/terms. https://doi.org/10.1017/CBO9781107706620.010

we immediately conclude that

$$\int d^4\chi_A d^4\chi_B\, [A, B, 3, 4, 1] \times [\hat{B}, 1, 2, 3, \hat{4}] = 0\,. \tag{7.68}$$

In the next case, $[\hat{B}, 1, 2, \hat{4}, A]$, we have $\delta^{(4)}(\chi_{\hat{B}}\langle 12\hat{4}A\rangle + \chi_A\,\langle \hat{B}12\hat{4}\rangle + \cdots)$. As before the $\chi_{\hat{B}}$-term can be dropped. Moreover, one can show that $\langle \hat{B}12\hat{4}\rangle$ vanishes (see Exercise 7.7 below), so we conclude

$$\int d^4\chi_A d^4\chi_B\, [A, B, 3, 4, 1] \times [\hat{B}, 1, 2, \hat{4}, A] = 0\,. \tag{7.69}$$

▶ **Exercise 7.7**

The 3-term Schouten identity (2.48) for angle and square spinors is the statement that three vectors in a plane are linearly dependent. As 4-component objects, the momentum twistors Z^I, $I = (\dot{a}, a)$, similarly satisfy a 5-term Schouten identity,

$$\langle i, j, k, l\rangle Z_m + \langle j, k, l, m\rangle Z_i + \langle k, l, m, i\rangle Z_j + \langle l, m, i, j\rangle Z_k + \langle m, i, j, k\rangle Z_l = 0\,. \tag{7.70}$$

Use (7.70) to derive the two identities

$$\langle \hat{B}12\hat{4}\rangle = 0\,, \qquad \langle 234\hat{B}\rangle = -\frac{\langle 1234\rangle\langle 34AB\rangle}{\langle A341\rangle}\,. \tag{7.71}$$

Hint: $\langle AB\hat{4}1\rangle = 0$; this identity follows from (7.65).

With the help of the second identity in (7.71), one finds that the result of integrating the $\delta^{(4)}$s in $[A, B, 3, 4, 1] \times [\hat{B}, 2, 3, \hat{4}, A]$ gives $\langle 1234\rangle^4\langle 34AB\rangle^4$.

In conclusion, after Grassmann integration, only the third 5-bracket in (7.64) contributes. After some simplifications one finds

$$\int d^4\chi_A d^4\chi_B\, [A, B, 3, 4, 1] \times [\hat{B}, 2, 3, \hat{4}, A] = \frac{\langle 1234\rangle\langle AB34\rangle}{\langle A234\rangle\langle B341\rangle} \times I_4(A, B)\,, \tag{7.72}$$

where

$$I_4(A, B) = \frac{\langle 1234\rangle^2}{\langle AB12\rangle\langle AB23\rangle\langle AB34\rangle\langle AB41\rangle}\,. \tag{7.73}$$

▶ **Exercise 7.8**

Derive (7.72).

$I_4(A, B)$ is the answer we expect, cf. (7.59), so now we have to massage its prefactor in (7.72). The recursion relations (7.63) instruct us to perform the forward limit by evaluating the $GL(2)$ integral:

$$\mathcal{A}_4^{\text{1-loop}} = \mathcal{A}_{4,\text{MHV}}^{\text{tree}} \int \frac{d^4Z_A d^4Z_B}{\text{Vol}[GL(2)]} \int_{GL(2)} I_4(A, B) \times \frac{\langle 1234\rangle\langle AB34\rangle}{\langle A234\rangle\langle B341\rangle}\,. \tag{7.74}$$

Downloaded from https://www.cambridge.org/core. UNIVERSIDAD AUTONOMA METROPOLITANA, on 14 Nov 2026 at 01:30:40, subject to the Cambridge Core terms of use, available at https://www.cambridge.org/core/terms. https://doi.org/10.1017/CBO9781107706620.010

This can be done by first making a $GL(2)$ rotation (7.55) of Z_A, Z_B and then integrating over the $GL(2)$ parameters. Since the integral is $GL(1)$ invariant, we can fix the scale in the $GL(2)$ matrix and set $c_{A'}{}^{A} = c_{B'}{}^{B} = 1$. With this "gauge fixing," we have

$$\begin{pmatrix} Z_A \\ Z_B \end{pmatrix} \to \begin{pmatrix} 1 & c_{A'} \\ c_{B'} & 1 \end{pmatrix} \begin{pmatrix} Z_A \\ Z_B \end{pmatrix}. \tag{7.75}$$

The result of this transformation on the 4-brackets is

$$\begin{aligned} \langle ABij\rangle \to \langle ABij\rangle\langle c_{A'}c_{B'}\rangle\,, \qquad & \langle Aijk\rangle \to \langle Aijk\rangle + c_{A'}\,\langle Bijk\rangle\,, \\ & \langle Bijk\rangle \to c_{B'}\,\langle Aijk\rangle + \langle Bijk\rangle\,, \end{aligned} \tag{7.76}$$

and the gauge fixing means that $\langle c_{A'}c_{B'}\rangle = 1 - c_{A'}c_{B'}$. Also, $\langle c_{A'}dc_{A'}\rangle = dc_{A'}$ and $\langle c_{B'}dc_{B'}\rangle = dc_{B'}$. So including the appropriate $GL(2)$ measure (7.57), we have

$$\begin{aligned} \mathcal{A}_4^{\text{1-loop}} = \mathcal{A}_{4,\text{MHV}}^{\text{tree}} \int \frac{d^4Z_A d^4Z_B}{\text{Vol}[GL(2)]}\, I_4(A,B)\,\langle 1234\rangle\langle AB34\rangle \\ \times \int \frac{dc_{A'}\,dc_{B'}}{\Big(1 - c_{A'}c_{B'}\Big)\Big(\langle A234\rangle + c_{A'}\,\langle B234\rangle\Big)\Big(c_{B'}\,\langle A341\rangle + \langle B341\rangle\Big)}\,. \end{aligned} \tag{7.77}$$

Now the plan all along was that the $GL(2)$ integration was supposed to localize us on the forward limit. So consider the denominator factor $(c_{B'}\,\langle A341\rangle + \langle B341\rangle)$. The vanishing of this expression is the statement that $\hat{Z}_B = Z_B + c_{B'}Z_A$ is sent to the intersection point of the line (A, B) and the plane $(3, 4, 1)$: but this is exactly part of the forward limit $\hat{Z}_B \to Z_{\hat{B}} = (A, B)\bigcap(3, 4, 1)$. So to realize this, we take the contour (7.77) in the $c_{B'}$-plane to surround the pole $c_{B'*} = -\langle B341\rangle/\langle A341\rangle$. Now we also want to send A to the intersection point $\hat{B}$, but the integral (7.77) appears not to have a pole that achieves this. However, when we evaluate the $c_{B'}$-integral to localize $B \to \hat{B}$, the factor $(1 - c_{A'}c_{B'})$ actually develops the desired pole, namely $c_{A'*} = -\langle A341\rangle/\langle B341\rangle$. Just do it:

$$\begin{aligned} &\int_{\mathcal{C}(c_{A'*})} dc_{A'} \int_{\mathcal{C}(c_{B'*})} dc_{B'}\, \frac{1}{\Big(1 - c_{A'}c_{B'}\Big)\Big(\langle A234\rangle + c_{A'}\,\langle B234\rangle\Big)\Big(c_{B'}\,\langle A341\rangle + \langle B341\rangle\Big)} \\ &= \int_{\mathcal{C}(c_{A'*})} \frac{dc_{A'}}{\Big(\langle A341\rangle + c_{A'}\langle B341\rangle\Big)\Big(\langle A234\rangle + c_{A'}\,\langle B234\rangle\Big)} \\ &= \frac{1}{\langle A234\rangle\langle B341\rangle + \langle A341\rangle\,\langle B234\rangle} \\ &= -\frac{1}{\langle AB34\rangle\langle 1234\rangle}\,. \end{aligned} \tag{7.78}$$

In the last line we used the 5-term Schouten identity (7.70). Plugging this result into (7.77), the factors $\langle AB34\rangle\langle 1234\rangle$ cancel and we are left with

$$\mathcal{A}_4^{\text{1-loop}} = -\mathcal{A}_{4,\text{MHV}}^{\text{tree}} \int \frac{d^4Z_A d^4Z_B}{\text{Vol}[GL(2)]}\, I_4(A,B)\,. \tag{7.79}$$

This is the correct result, as we discussed in Section 7.4.

Downloaded from https://www.cambridge.org/core. UNIVERSIDAD AUTONOMA METROPOLITANA, on 14 Nov 2026 at 01:30:40, subject to the Cambridge Core terms of use, available at https://www.cambridge.org/core/terms. https://doi.org/10.1017/CBO9781107706620.010

Note that in this derivation, the $GL(2)$ integral ended up localizing the integrand on the forward limit, where the poles that were used in this localization were given by the extra $[A, B, 3, 4, 1]$. This precisely realizes the idea we described around (7.60). Now you might be a little concerned that we could have chosen to localize on "non-forward" poles in the $GL(2)$ integral instead, but the answer would have been the same, as guaranteed by the large-$c_{A',B'}$ falloff of the integrand.

Finally, you may find it discouraging that it takes much more work and sophistication to calculate even the simplest of all $\mathcal{N} = 4$ SYM amplitudes with BCFW than it did with the generalized unitarity method, as we showed in Section 6.2. However, while it is not directly practical, it is morally encouraging – and perhaps even fascinating – that all information about the 4-point MHV 1-loop amplitude is encoded already in the 6-point NMHV tree-level amplitude. This is a realization of an interesting connection between amplitudes with different numbers of particles n, different $\mathrm{N}^K\mathrm{MHV}$ levels, and different loop-orders L.

7.6 Higher loops

The planar loop-integrand recursion relations studied above can also be directly applied to higher-loop order in the planar limit of $\mathcal{N} = 4$ SYM. This was already shown in (7.61). However, in contrast to the unitarity approach, the integrands obtained from recursion generally contain spurious poles. Local poles (non-spurious) refer to propagator-like poles, these take the form of $1/\langle i, i-1, j, j-1\rangle$ or $1/\langle A, B, i-1, i\rangle$ in momentum twistor space. Spurious poles, on the other hand, could take the form $1/\langle A, B, 4, 2\rangle$; this is non-local in that it does not arise from a propagator in the loop-diagrams. At 4-point, since there is only one term in the recursion, such spurious poles must vanish by themselves, and indeed the final result is free of spurious poles. However, at higher-points the spurious poles cancel between various terms in the recursion relations, but their presence in the individual BCFW terms makes it difficult to carry out the integration of the loop-integrand to obtain the actual amplitude. Spurious poles are a hallmark of BCFW recursion relations – we discussed this for tree-level BCFW at the end of Section 3.2. BCFW builds in unitarity and gauge-invariance at the expense of manifest locality. While it provides us with a method to compute loop-integrands, it leads to complications as one eventually has to integrate these non-local functions in momentum space.

Given the large amount of symmetry enjoyed by $\mathcal{N} = 4$ SYM – superconformal symmetry and dual conformal symmetry as well as their enhancement to the Yangian – it is tempting to be ambitious and ask if it is possible to manifest *both* locality and dual conformal invariance at the same time. Certainly the unitary method discussed previously would suffice for this purpose, since the dual conformal invariant scalar integrals are local. However, when extended beyond 4-point, the number of dual conformal invariant integrals becomes large and not all of them may contribute to a given amplitude.

At 1-loop level, the 1-loop box integral in (7.59) is the only available dual conformal invariant local 4-point integral. In other words, dual conformal symmetry forces the triangle

Downloaded from https://www.cambridge.org/core. UNIVERSIDAD AUTONOMA METROPOLITANA, on 14 Nov 2026 at 01:30:40, subject to the Cambridge Core terms of use, available at https://www.cambridge.org/core/terms. https://doi.org/10.1017/CBO9781107706620.010

and bubble-contributions to be absent in $\mathcal{N} = 4$ SYM. Could it be that all amplitudes $\mathcal{N} = 4$ SYM are fixed by similar considerations? To study this involves *maximal cuts* and *Leading Singularities* – and some of the principles involved also extend beyond the planar limit and to SYM with less supersymmetry. We introduce the basic setup in the following chapter.

Downloaded from https://www.cambridge.org/core. UNIVERSIDAD AUTONOMA METROPOLITANA, on 14 Nov 2026 at 01:30:40, subject to the Cambridge Core terms of use, available at https://www.cambridge.org/core/terms. https://doi.org/10.1017/CBO9781107706620.010